A Proof of Theorem 1

We now provide a proof of Theorem 1 which states that the quality of the approximation of $v^{(t+2)}$ is improved by one error order when the extrapolation step (11d) is added after the velocity update step.

Proof. If we remove the extrapolation step (11d) from Algorithm 1, Taylor's Theorem implies that $v^{(t+1)}$ yields an estimator of error order $\mathcal{O}(\tau)$ for the velocity in the next timestep $v^{(t+2)}$:

$$v^{(t+2)} = v^{(t+1)} + \mathcal{O}(\tau). \tag{14}$$

The standard backward distance approximation provides an estimation of $\dot{v}^{(t+1)}$:

$$\dot{v}^{(t+1)} = \frac{v^{(t+1)} - v^{(t)}}{\tau} + \mathcal{O}(\tau). \tag{15}$$

Combining this with a Taylor expansion of $v^{(t+2)}$ then yields the statement from the Theorem:

$$v^{(t+2)} = v^{(t+1)} + \tau\dot{v}^{(t+1)} + \mathcal{O}(\tau^2) = v^{(t+1)} + \tau\frac{v^{(t+1)} - v^{(t)}}{\tau} + \mathcal{O}(\tau^2) = \tag{16}$$

$$2v^{(t+1)} - v^{(t)} + \mathcal{O}(\tau^2) = \bar{v}^{(t+1)} + \mathcal{O}(\tau^2). \tag{17}$$

B Runtime analysis

We compare the runtime of our method to other popular shape interpolation methods based on our experiments on TOSCA in Figure 11. Only divergence-free interpolation [19] is faster than our method. Most importantly, for our approach and [19] the runtime is essentially independent of the resolution because the optimization is done on a fixed resolution of 2k vertices. Only the last forward pass on the whole input shape $p \in \mathbb{R}^{n\times 3}$ depends on the resolution n but this step is cheap in comparison to the optimization.

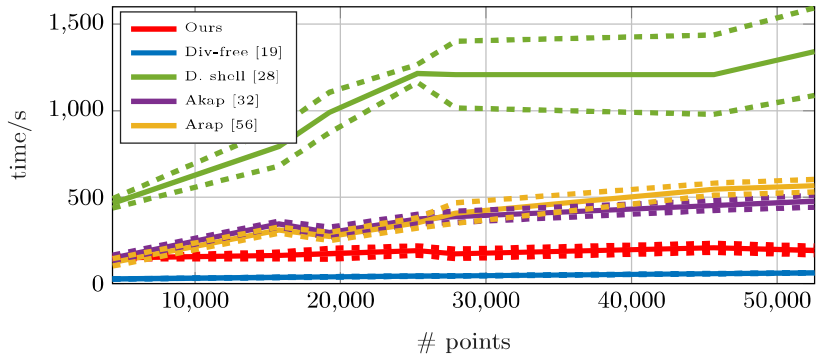

Fig. 11. A runtime analysis of different interpolation methods on all pairs in TOSCA. We plot the mean computation time (solid line) and two lines corresponding to one standard deviation (dashed).

C Additional qualitative evaluations

To give a more complete picture, we show additional examples of interpolations with our method on the two datasets with reals scans, SHREC'19 Isometry and FAUST in Figure 12 and Figure 13. Finally, we show a failure case under topological changes on a scanned hand from SHREC'19 in Figure 14. Although our method is not able to separate the touching parts for these cases, our method still produces a more plausible result than other classical interpolation methods. In our case, the fingers appear to be glued together whereas [28] produces undesirable artifacts.

Fig. 12. Additional examples of interpolations with our method on SHREC'19.

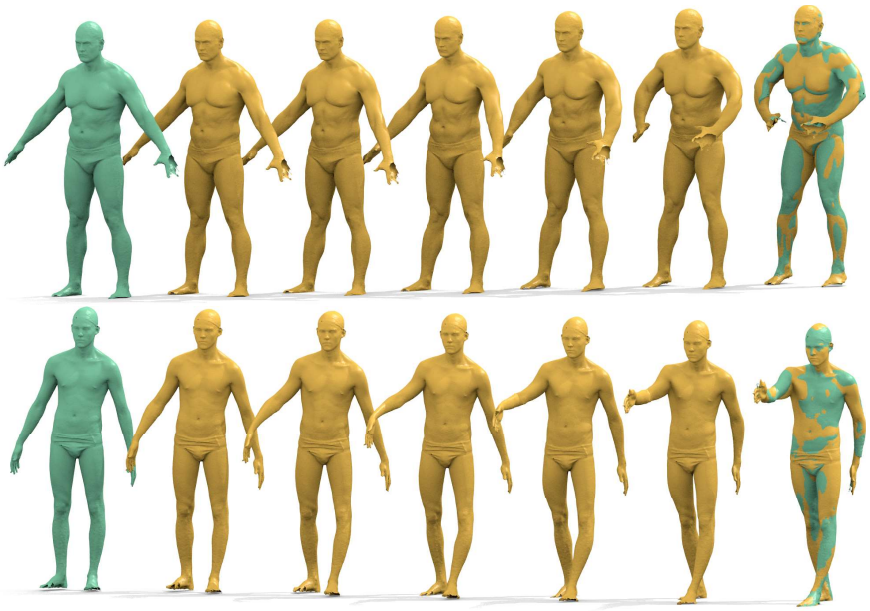

Fig. 13. Additional examples of interpolations with our method on FAUST.

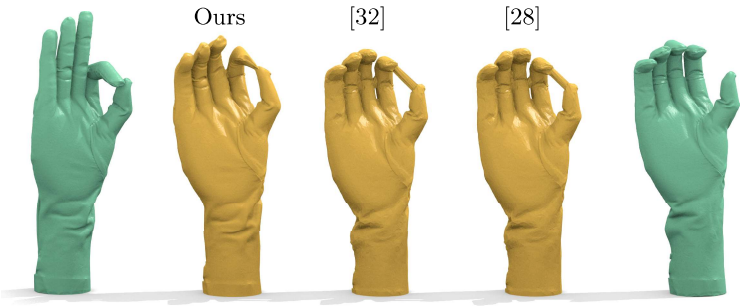

Fig. 14. An example of a scanned hand from SHREC'19 Isometry [17] where we show the second to last frame from our method, [28] and [32] respectively. In SHREC'19 there are various pairs with topological changes. In the case presented here, the meshing connects between the index finger and the thumb. This makes our method fail because the input matching from [20] is not able to separate the two fingers entirely.

D Ablation study

We present an ablation study in order to assess how the different components of our pipeline contribute to the quantitative results in Fig. 7. In particular, we perform the following ablations:

i. Replacing the anisotropic arap energy (9) with the standard arap energy (1).
ii. Removing the extrapolation step (11d).
iii. Removing the regularization term in Equation (13).

See Table 1 for a summary of the quantitative results for these configurations on TOSCA and SCAPE. For each experiment, we report the error of the different metrics, averaged over all pairs in the dataset.

TOSCA	(i.) Isotropic arap	(ii.) No extrapolation	(iii.) No regularization	Ours
Conformal dist.	0.7413	0.4284	2.8234	0.3626
Rel. volume ch.	5.4e-06	1.6e-05	3.0e-02	5.4e-06
Chamfer dist.	0.0122	0.0057	0.0083	0.0051
SCAPE	(i.) Isotropic arap	(ii.) No extrapolation	(iii.) No regularization	Ours
Conformal dist.	0.8882	0.4678	2.7270	0.3857
Rel. volume ch.	1.3e-05	3.8e-05	2.7e-02	6.7e-06
Chamfer dist.	0.0140	0.0076	0.0059	0.0066

Table 1. The results of our ablation study, see Appendix D for more details.